Physica A 388 (2009) 1687–1695

Contents lists available at ScienceDirect

Physica A

journal homepage: www.elsevier.com/locate/physa

On the detection of trends in long-term correlated records

Diego Rybski [a,b,*], Armin Bunde [a]

[a] Institut für Theoretische Physik III, Justus-Liebig-Universität Giessen, 35392 Giessen, Germany
[b] Levich Institute and Physics Department, City College of New York, New York, NY 10031, USA

ARTICLE INFO

Article history:
Received 1 November 2008
Available online 16 December 2008

PACS:
05.40.-a
24.60.-k
43.60.Wy
52.25.Gj
92.05.Ek
92.60.Ry
92.70.Gt

Keywords:
Trends
Long-term correlations
Detection
Climate
Temperature
Detrended fluctuation analysis

ABSTRACT

We use the Detrended Fluctuation Analysis (DFA) to quantify underlying trends in long-term correlated records. Our approach is based on the fact that different orders of DFA are affected differently by trends. For a given instrumental record of length N, we compare the fluctuation exponent α_0 of DFA0 where trends are not being eliminated, with the fluctuation exponent α_2 of DFA2 where possible linear trends in the instrumental record are being eliminated. From this we deduce numerically the probability density $p(A)$ that in the considered long-term correlated record, a linear trend with a slope between A and $A + \mathrm{d}A$ occurs. Without loss of generality we focus on Gaussian distributed data. As an example, we apply our analysis to several long temperature records (Melbourne, Oxford, Prague, Pusan, Uppsala, and Vienna), where we discuss the trends within the last 90 years, which may originate from both, urban and global warming.

1. Introduction

Long-term correlations have been first observed by H.E. Hurst, who found “long-range statistical dependencies” [1] in river-runoff records, and mathematically described by Mandelbrot [2,3]. In the last decades it has become clear that long-term correlations are abundant in nature, characterizing, for example, temperature records [4–12], hydrological records [2,3,13,14], physiological records [15,16], economic records (for reviews, see, e.g. Refs. [17,18]) and even records of human activity [19,20]. In long-term correlated records, large events well above the average are more likely to be followed by large events, and small events well below the average by small events. This persistence occurs on all time scales. For example, a week where the temperature is high, is more likely to be followed by a warm week than by a cold week, a warm month is more likely followed by a warm month than by a cold one, and the same holds on annual and decadal scales, and probably even on centennial scales [12,21]. This persistence on all scales is characterized by an autocorrelation function that decays in time by a power law, $C(s) \sim s^{-\gamma}$ with an exponent γ between 0 and 1. One of the consequences, of the pronounced mountain–valley-structure is the clustering of extreme events in time [22,23] where periods of short return times are followed by periods of large return times.

Since large mountain and valley epochs may look like positive and negative trends (see Fig. 1), it is generally difficult to distinguish between long-term correlated and deterministic trendy behavior. One of the major challenges here is the

* Corresponding author at: Institut für Theoretische Physik III, Justus-Liebig-Universität Giessen, 35392 Giessen, Germany.
E-mail address: ca-dr@rybski.de (D. Rybski).

doi:10.1016/j.physa.2008.12.026

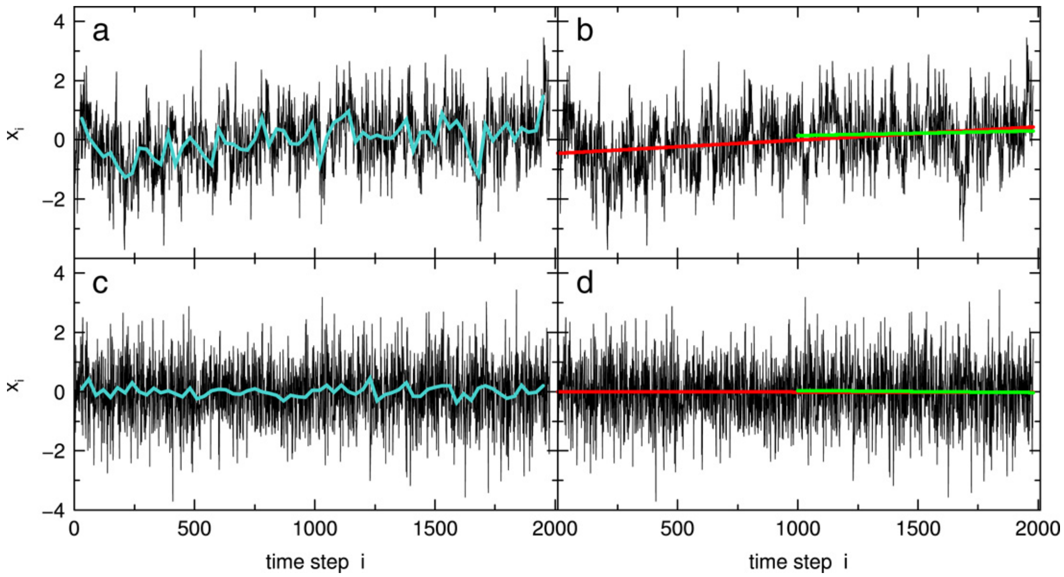

Fig. 1. Mountain–valley-structure of long-term correlated records. (a, b) an artificial example with fluctuation exponent $\alpha = 0.85$ ($\gamma = 0.3$) (c, d) randomly shuffled values, destroying any correlations. In order to emphasize the long-term behavior, the thick lines in (a, c) represent down-sampled values in windows of size 30. The straight lines in (b, d) are least square fits to the records using different periods (red: total; green: starting from 1000). One can see, that due to the mountain–valley-structure of long-term correlated records steeper slopes are more likely to occur. The record in (a, b) was created using Fourier filtering, see e.g. Ref. [24]. (For interpretation of the references to colour in this figure legend, the reader is referred to the web version of this article.)

detection- and attribution problem in climatology. The question is, how much of the recent increase in the temperature of the earth's atmosphere and hydrosphere (which are long-term correlated) can be attributed to natural fluctuations, and how much is of anthropogenic origin [25,21]. Currently, there exist several techniques (like the Detrended Fluctuation Analysis or the Wavelet Technique) that are able to systematically eliminate trends in the presence of long-term correlations, but there is no conclusive method available that allows to eliminate the fluctuations and then obtain the trend. In short-term correlated records with a finite correlation time $s_\times$, the correlations can be eliminated by down-sampling, i.e. averaging them over time windows that are considerably larger than the correlation time. But since in long-term correlated sequences the correlation time is, in principle, infinite, this kind of filtering cannot be applied.

Here we present a method that is based on an extension of the Detrended Fluctuation Analysis (DFA) [26] as suggested in Ref. [16] (see also Refs. [24,27,28]). Our approach is based on the fact that different orders of DFA are affected differently by trends, which we use to obtain (for a given long-term correlated record of length N) the probability density $p(A)$ that a linear trend with a slope between A and $A + \mathrm{d}A$ occurs. As an example, we apply our analysis to several long temperature records (Melbourne, Oxford, Prague, Pusan, Uppsala, and Vienna).

The paper is organized as follows. In Section 2 we briefly describe long-term correlations and the Detrended Fluctuation Analysis. In Section 3 we describe our trend estimation method, which we then apply in Section 4 to the temperature records. In Section 5 we summarize the results and draw our conclusions.

2. Long-term correlations and trends

2.1. Elimination of seasonal trends

We consider a record (T_i) of $i = 1, \ldots, N$ equidistant measurements. In most hydro-climate applications, the index i will correspond to days or years.

We assume that the record can be approximated well by a superposition of 3 components,

$$T_i = x_i + y_i + z_i, \tag{1}$$

where x_i is the (correlated) noise component ($\langle x \rangle = 0$), y_i the trend component, and z_i is the periodic component.

To eliminate the periodic component, one usually concentrates on the departures

$$w_i := T_i - \langle T \rangle_{i \bmod \lambda} \tag{2}$$

from the periodic mean, with λ being the period. In the case of daily temperatures, $\lambda = 365$ and the values $\langle T \rangle_{i \bmod \lambda}$ are simply the mean temperatures for each calendar date, e.g. 2nd of March, obtained by averaging over all years in the record. Thus, in the following we focus on the record w_i, $w_i \simeq x_i + y_i$, that only contains a noise and trend component. Without loss of generality we will assume that the w_i have zero mean.

2.2. Detrended fluctuation analysis (DFA)

The Detrended Fluctuation Analysis (DFA) is a well-established method for determining the scaling of long-term correlations in the presence of trends without knowing their origin and shape [26,29,16,24,30]. Long-term correlated records are characterized by an autocorrelation function

$$C(s) = \frac{\langle x_i x_{i+s} \rangle}{\langle x^2 \rangle} = \frac{1}{(N-s)\langle x^2 \rangle} \sum_{i=1}^{N-s} x_i x_{i+s} \tag{3}$$

that declines algebraically with the time lag s,

$$C(s) \sim s^{-\gamma}. \tag{4}$$

The correlation exponent γ is between 0 and 1, such that the mean correlation time $\bar{s} = \int_0^\infty C(s) \mathrm{d}s$ diverges. For $\gamma > 1$, the data are only short-term correlated, since $\bar{s}$ remains finite. In general, the direct calculation of $C(s)$ is severely affected by finite size effects (shortness of the record) and by the presence of trends.

The DFA depends less on finite size effects and can eliminate systematically polynomial trends. In DFA, one considers the cumulative sum ("profile") of the w_i and studies its fluctuations around polynomial best fits in time windows of size s. If we choose for the polynomial a constant (0-order) polynomial, we call the procedure DFA0. In general, if we choose an nth order polynomial, we call it DFAn. In this paper, we will focus exclusively on DFA0 and DFA2.

In general, the DFA procedure consists of three steps:

(1) Determine the profile:

$$Y(i) = \sum_{k=1}^{i} w_k, \tag{5}$$

of the (deseasoned) record (w_i) of length N and cut it into $N_s = \mathrm{int}(N/s)$ non-overlapping segments of equal length s (an illustrative Figure can be found, e.g., in Ref. [24]).

(2) In each of these segments ν, determine the local polynomial trend (of given order n) by a least-square fit and determine the variance $F_s^2(\nu)$ around it.

(3) Average over all segments and take the square root to obtain the DFAn fluctuation function:

$$F^{(n)}(s) = \left[\frac{1}{N_s} \sum_{\nu=1}^{N_s} F_s^2(\nu) \right]^{1/2}. \tag{6}$$

For different detrending orders n one obtains different fluctuation functions $F^{(n)}(s)$. For long-term correlated data without deterministic trend, the $F^{(n)}(s)$ all scale the same,

$$F^{(n)}(s) \sim s^{\alpha_n} \tag{7}$$

with

$$\alpha_n = \begin{cases} 1 - \gamma/2 & \text{for } 0 < \gamma \le 1 \\ 1/2 & \text{for } \gamma > 1. \end{cases} \tag{8}$$

By definition, DFAn eliminates trends of order n in the profile which represent trends of order $n-1$ in the original record. Thus, in the presence of a linear trend in the original data, DFA0 and DFA1 are influenced by the trend and do not scale according to Eq. (7), while DFA2, DFA3, etc. do so. It has been suggested in Ref. [24] that this feature can be utilized for a trend detection in the presence of long-term correlations. In this paper we follow this path. For simplicity we focus on linear trends in the original data. In this case, DFA0 asymptotically scales as $F^{(0)}(s) \sim s$, i.e., $\alpha_0 \to 1$, while DFA2 removes the trend and scales as $F^{(2)}(s) \sim s^{\alpha}$, i.e., $\alpha_2 \simeq \alpha$. For finite records and small trends, the asymptotic behavior of DFA0 cannot be observed, and its fluctuation function scales effectively as $F^{(0)}(s) \sim s^{\alpha_0}$ with $1 \ge \alpha_0$. The discrepancy between the effective exponent α_0 and the exponent α_2 is our main indicator for the trend. But when evaluating the trend this way one has to bear in mind that due to the squares in Eq. (6), increasing and decreasing trends lead to the same effective exponent α_0.

We like to note that for stationary mono-fractal time series [31], α_1 corresponds to the classical Hurst exponent H determined by Rescaled Range Analysis [1,32]. DFA0 is equivalent to the simplest Fluctuation Analysis (FA) [33,6] and identical to the aggregated standard deviation method (ASD), see e.g. Ref. [34]. Finally, when applying standard spectral analysis techniques to a long-term correlated record without a trend, the power spectrum $S(f)$ scales with frequency f as $S(f) \sim f^{-\beta}$, where β is related to the fluctuation exponent α by $\beta = 2\alpha - 1$, see, e.g., Refs. [35–37].

3. Trend estimation with Detrended Fluctuation Analysis

In the following, we describe a method to evaluate a deterministic trend in a given record that is superimposed on long-term correlated fluctuations characterized by the fluctuation exponent α. We assume that the trend is weak and can be approximated by a linear function $y_i = A(i - \frac{N}{2})$.

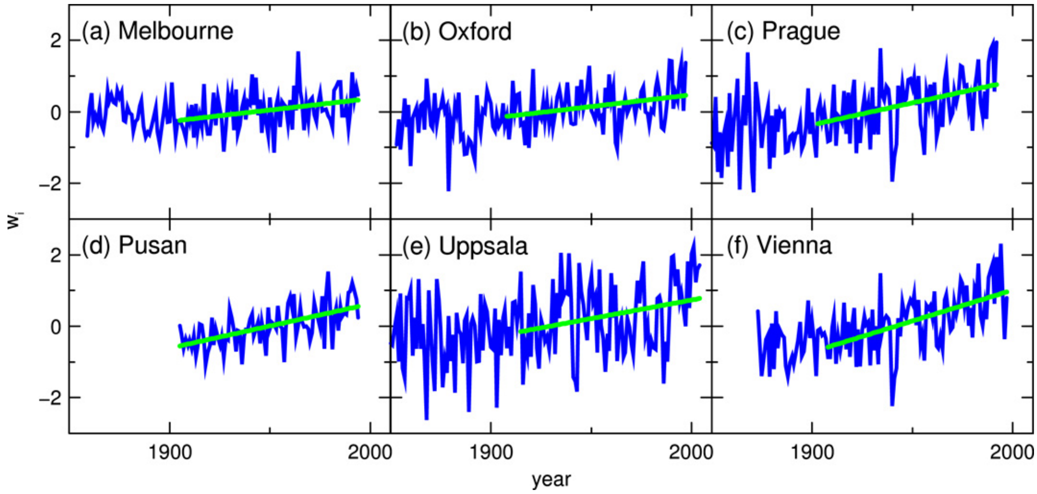

Fig. 2. Considered temperature records plotted in annual resolution. (a) Melbourne (AUS, 1859–1994), (b) Oxford (GBR, 1853–1997), (c) Prague (CZE, 1775–1992), (d) Pusan (KOR, 1904–1994, 90 years and 8 months), (e) Uppsala (SWE, 1722–2004 [38,39]), and (f) Vienna (AUT, 1873–1997). The straight lines are least square fits to the last 90 years of the records.

In our approach, we use Monte-Carlo simulations and generate a large number of records (with given N, α, and A values). We request that each record follows, in the considered time frame, the same (upward or downward) tendency as the measured record, described by increasing or decreasing regression lines (positive or negative sign). In the temperature records considered here, the regression lines are always increasing, see Fig. 2. The question we ask is, what is the probability density that the slope of the linear trend is between A and $A + \mathrm{d}A$. To answer this question numerically, we perform the following steps:

(1) Apply DFA0 and DFA2 to the considered record of length N and determine the values of the exponents α_0^* and α_2^* by power-law fits from the fluctuation functions.
(2) Use the Fourier filtering method (see e.g. Ref. [24]), where the same fluctuation exponent $\alpha = \alpha_2^*$ as the considered record is imposed, to create a large number of synthetic records with the same length N.
(3) Apply DFA2 to the synthetic records. Keep only those K records where the exponent α_2 is between $\alpha_2^* - \delta$ and $\alpha_2^* + \delta$. Reject all others configurations.
(4) Apply DFA0 and determine, for each of the K remaining records, the DFA0 exponent α_0.
(5) Count the number $R_{\alpha_0^*}$ of configurations where
   - α_0 is between $\alpha_0^* - \delta$ and $\alpha_0^* + \delta$, and
   - the slope of a linear regression has the same sign as the considered real record.
(6) Add a linear trend with slope A to the accepted K records [see step (3)] and repeat the steps (4–6).

By varying A, we obtain the histogram $R_{\alpha_0^*}(A)$, and by normalizing it, we arrive at an estimate for the final probability $p_\delta(A)$ that the considered record has a trend with slopes between A and $A + \mathrm{d}A$. Accordingly, by plotting $p_\delta(A)$ against A, we can estimate the trend that most likely leads to the DFA0- and DFA2-slopes α_0^* and α_2^* characterizing the record. Since the maximum slope of DFA0 is 1 [24], this method only works sufficiently well if the long-term correlations are not too strong (α_2^* has to be well below 1). If α_2^* is close to 1, no difference between DFA0 and DFA2 is found ($\alpha_0 \approx \alpha_2$), even when a (linear) trend is added. In this case we suggest to use the comparison of α_1 and α_2, which on the other hand requires rather stronger trends.

4. Application to temperature records

Fig. 2 shows (in annual resolution) the temperature records that we consider here. The figure also shows least square fits for the last 90 years (green), the period to which we restrict our study. It is the length of the shortest considered record (Pusan). Again, the question is how much of the increase in Fig. 2 can be attributed to the natural fluctuations (long-term correlations) and how much is the consequence of a trend in the sense of a deterministic change.

In order to reduce the influence of short-term correlations in the temperature records, that basically reflect the short-term persistence of the weather [9], we do not use daily resolution, but aggregate the records by averaging the data in non-overlapping windows of 12 days. Accordingly, the resulting aggregated records have length N that is 12 times shorter than the daily records.

In our analysis, we follow the steps described above (Section 3). First we apply DFA (here DFA0, DFA1, DFA2 and DFA3) to the records. The corresponding fluctuation functions are depicted in Fig. 3. The figure shows that DFA2 and DFA3 have

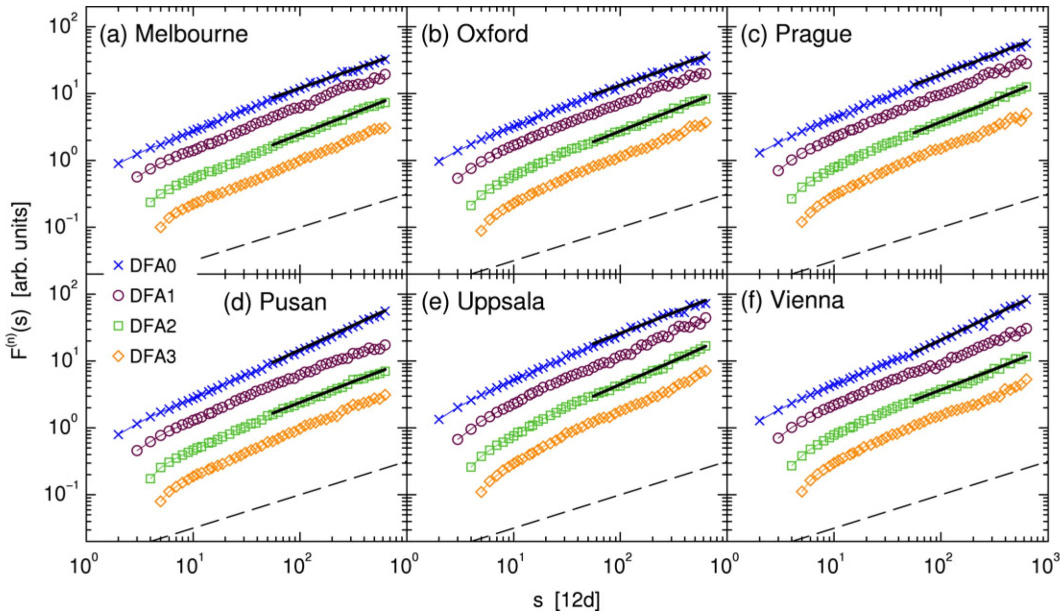

Fig. 3. Detrended Fluctuation Analysis of the considered temperature records shown in Fig. 2 for the last available 90 years. The panels exhibit the fluctuation functions obtained with DFA0–DFA3 (from top to bottom) plotted against the time scale. The thick solid lines represent the exponents (a) Melbourne, $\alpha_0^* = 0.56$, $\alpha_2^* = 0.63$; (b) Oxford, $\alpha_0^* = 0.67$, $\alpha_2^* = 0.64$; (c) Prague, $\alpha_0^* = 0.72$, $\alpha_2^* = 0.61$; (d) Pusan $\alpha_0^* = 0.74$, $\alpha_2^* = 0.62$; (e) Uppsala $\alpha_0^* = 0.64$, $\alpha_2^* = 0.63$; and (f) Vienna $\alpha_0^* = 0.75$, $\alpha_2^* = 0.62$ on the scales $50 < s < 700$. The dashed line at the bottom of each panel indicates the uncorrelated case of $\alpha = 0.5$.

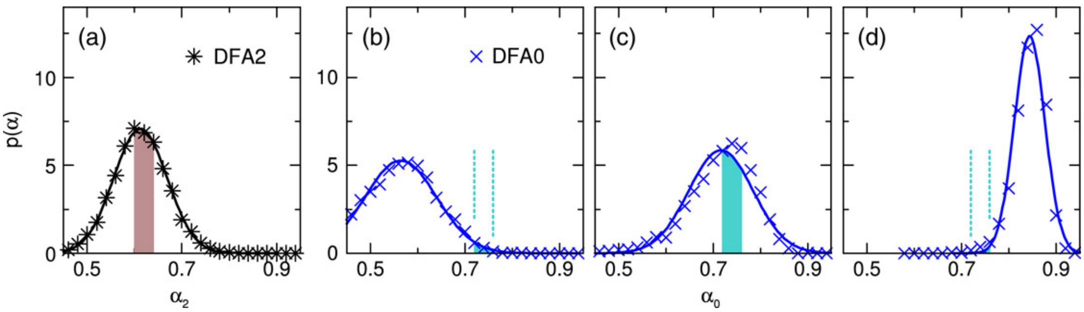

Fig. 4. Normalized histograms of the fluctuation exponents α_2 and α_0 determined from artificial records. Using Fourier filtering (see e.g. Ref. [24]) 10^4 records of length $N = 2756$ with imposed exponent $\alpha = 0.62$ were created. Panel (a, $*$, black) shows the exponents obtained by DFA2. After removing those sequences where α_2 is not in the range $0.62 - \delta < \alpha_2 < 0.62 + \delta$ [shaded area in (a)], a linear trend of slope A is added: (b) $A = 0\sigma/N$, (c) $A = 0.5\sigma/N$, and (d) $A = 1.0\sigma/N$. The panels show the exponents α_0 (b–d, $\times$, blue) obtained by DFA0. The blue shaded areas in (b–d) represent the number of exponents α_0 found in $0.64 - \delta < \alpha_0 < 0.64 + \delta$. The solid lines, given by the corresponding normal distributions, are included for visualization only. The third condition (see step 5 in Section 3) requires increasing linear regressions (not shown). All exponents were determined in the time window $50 < s < 700$. (For interpretation of the references to colour in this figure legend, the reader is referred to the web version of this article.)

the same exponent (which indicates that trends have been removed completely by DFA2 in all 6 cases), while the exponent obtained by DFA0 is slightly larger (except for Melbourne).

Next, in step 2, we generate a large number of long-term correlated records with the same β-value by the Fourier filtering method. In step 3 we keep only those configurations that have concordant α_2-values. For the Pusan temperature record, for example, α_2 must be between $0.62 - \delta$ and $0.62 + \delta$. Fig. 4(a) shows the histogram of the fluctuation exponents determined with DFA2 for the synthetic sequences ($N = 2756$, imposed $\alpha = 0.62$). As expected, the histogram has a maximum at $\alpha_2^* = 0.62$. The shaded region in Fig. 4(a) represents the K approved configurations. In step 4, we then determine the DFA0-exponent α_0 for these remaining records, the distribution (for Pusan) is shown in Fig. 4(b). The figure depicts that the maximum occurs around $\alpha_0 = 0.55$ and thus is shifted slightly towards smaller values. This is an artefact of DFA0, which shows that due to considerable finite size effects (which are less pronounced for higher order DFA) the fluctuation exponents are underestimated and, in addition, spread considerably. Accordingly, contrary to the expectations, already the case $\alpha_0^* \simeq \alpha_2^*$ indicates some trend in a record (for an explanation of this effect, see Ref. [40]).

In the following steps 5 and 6, we add linear trends with slope A, count the number of configurations $R_{\alpha_0^*}(A)$ that (i) have exponents α_0 between $\alpha_0^* - \delta$ and $\alpha_0^* + \delta$ and (ii) have an increasing regression line. This condition is necessary to distinguish

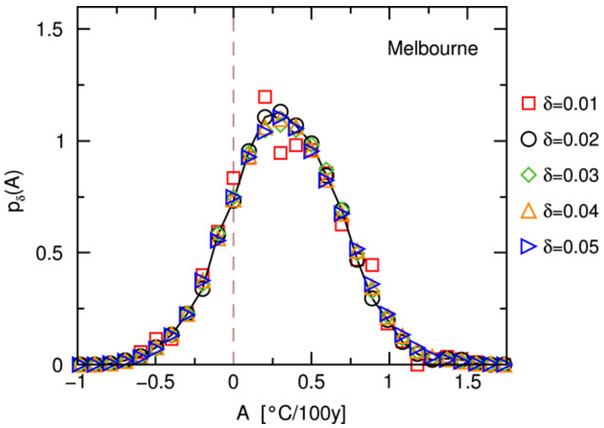

Fig. 5. Probability $p_\delta(A)$ that the slope of the trend is between A and $A + \mathrm{d}A$ as calculated comparing the DFA2 and DFA0-exponents obtained from the Melbourne-record and from synthetic records according to Section 3. The results are shown for different values of the parameter $\delta = 0.01 \ldots 0.05$. To transform the trend-values from the units σ/N to °C/100 years we consider the standard deviations of the instrumental records and of the artificial records with trends. The figure is based on 10^4 sequences with corresponding N and imposed α. The dashed vertical line indicates $A = 0$.

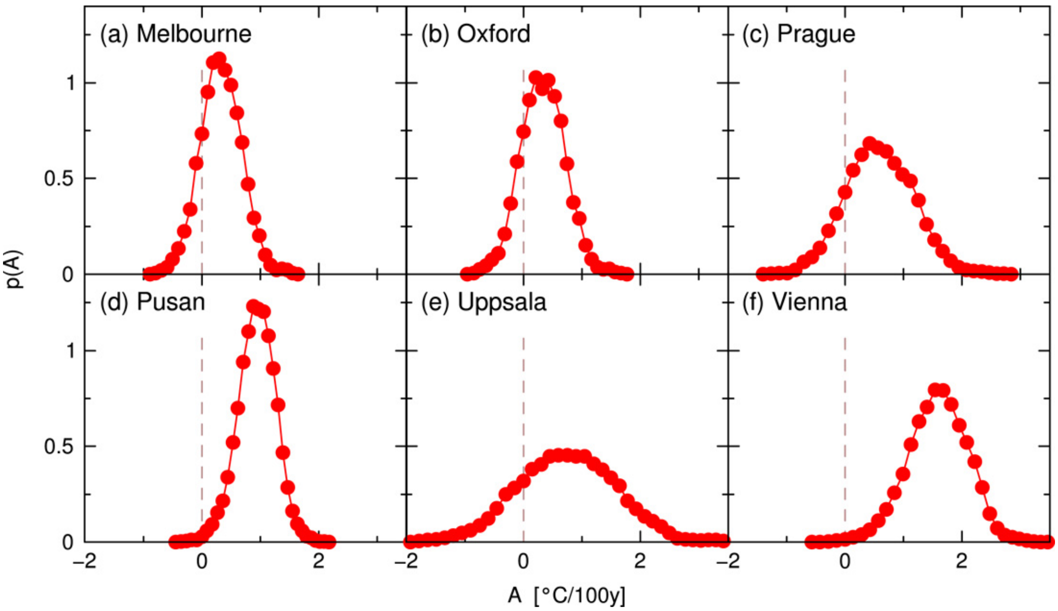

Fig. 6. Probability $p(A)$ that the slope of the trend is between A and $A+\mathrm{d}A$ as calculated comparing the DFA2 and DFA0-exponents. In the same arrangement as Fig. 3: (a) Melbourne, (b) Oxford, (c) Prague, (d) Pusan, (e) Uppsala, and (f) Vienna. To transform the trend-values from the units σ/N to °C/100 years we consider the standard deviations of the instrumental records and of the artificial records with trends. For each panel 10^4 sequences with corresponding N and imposed α have been generated. The dashed vertical lines indicate $A = 0$. As explained in the text, we restrict to $\delta = 0.02$.

between positive and negative A-values in $R_{\alpha_0^*}(A)$ —without it one would obtain $R_{\alpha_0^*}(|A|)$. For Pusan ($\alpha_0^* = 0.74$) the number of configurations $R_{\alpha_0^*}(A)$ is indicated by the shaded areas in Fig. 4(b–d), for three trend strengths A. $R_{\alpha_0^*}(A)$ is proportional to the probability $p_\delta(A)$ that the slope of the trend is between A and $A + \mathrm{d}A$. The proportionality constant is determined by the normalization condition. With increasing underlying trend [see Fig. 4(c,d)], the distribution of the DFA0-exponents is shifted towards larger values and becomes narrower. Fig. 5 exhibits $p_\delta(A)$ for the temperature record from Melbourne with δ ranging from 0.01 to 0.05. The data collapse in the figure shows that the outcome is practically independent of the tolerance δ. From now on we use $\delta = 0.02$ and skip this index in $p_\delta(A)$.

The resulting $p(A)$-curves for the six temperature records are depicted in Fig. 6. The most likely trend appears at the maximum of $p(A)$. By definition, $P(A) = \int_A^\infty p(A)\mathrm{d}A$ is the probability that the trend is larger than A. This probability is shown in Fig. 7. It also shows those A-values where $P(A) = 0.975$ or 0.025, which indicate the confidence levels $A_{0.975}$ and $A_{0.025}$. Between these levels, 95 % of all trends are found. Accordingly, the chance to have smaller or larger trends is 5 %.

As one can see in Fig. 6, the maxima at A_{typ} of the $p(A)$ curves occur always at positive A-values, which is due to the required increasing tendency (step 5 in Section 3). In Melbourne and Oxford, the trends are not significant since A_{typ} is

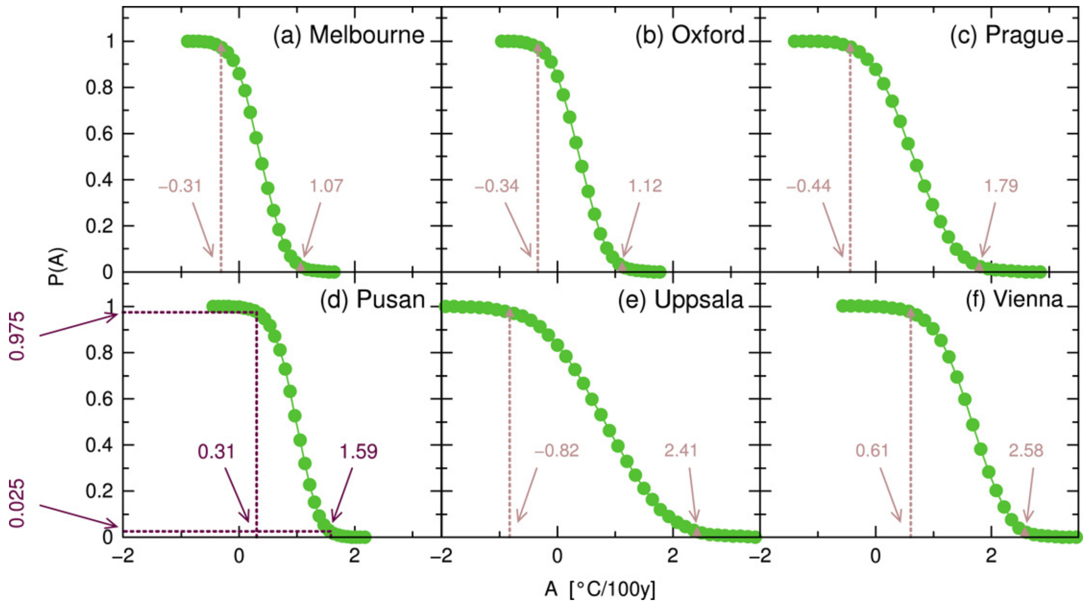

Fig. 7. Probability $P(A)$ that the slope of the trend is larger or equal to A. The values have been obtained integrating the curves from Fig. 6. In the same arrangement as Fig. 3: (a) Melbourne, (b) Oxford, (c) Prague, (d) Pusan, (e) Uppsala, and (f) Vienna. The arrows and dotted lines in (d) illustrate how the $A_{0.975}$ and $A_{0.025}$-values are determined.

Table 1
Overview of the results obtained with the proposed method and comparison with least square fits. For the studied examples (compare Fig. 2) we list the results for the last 90 years. The left part shows the results of the approach we propose and the right part shows the results of the least square fits. A_{typ} is the most likely trend, while $A_{0.975}$ and $A_{0.025}$ are the confidence levels including 95%. In the case of the DFA-based technique, they have been extracted from the $p(A)$- and $P(A)$-values (Figs. 6 and 7), while in the case of the least square fits, a bootstrapping technique (10^4 random samples with replacement) [41] has been used. All values are in units °C/100 years.

	Proposed method			Linear regression		
	$A_{0.975}$	A_{typ}	$A_{0.025}$	$A_{0.975}$	A_{typ}	$A_{0.025}$
Melbourne	−0.31	0.33	1.07	0.39	0.64	0.91
Oxford	−0.34	0.34	1.12	0.40	0.67	0.96
Prague	−0.44	0.60	1.79	0.97	1.31	1.67
Pusan	0.31	0.95	1.59	1.08	1.30	1.53
Uppsala	−0.82	0.76	2.41	0.75	1.15	1.53
Vienna	0.61	1.60	2.58	1.34	1.70	2.05

lower than the width ΔA of $p(A)$, while for Pusan and Vienna A_{typ} is considerably larger than ΔA. Table 1 summarizes the results of the proposed trend-detection method and compares them with the results from the conventional linear regression analysis where long-term correlations have not been taken explicitly into account. In the linear regression analysis, one applies least square fitting to obtain the regression lines. The most likely trends A_{typ} are simply given by the least square fit. The 2.5%-quantiles (95% confidence interval) were calculated using a bootstrapping technique (10^4 random samples with replacement) [41].

The table shows that in all cases the conventional regression analysis yields larger trends A_{typ} with confidence intervals that are considerably smaller than in the method we propose, exaggerating the trend and indicating a seemingly smaller uncertainty. Both features, however, are probably caused by the fact that the regression analysis is not able to take into account the long-term correlations in a proper way.

We would like to note, that we obtain similar results, when we use conventional Fluctuation Analysis (FA) [33,6] replacing DFA0, or when monthly resolution instead of 12 day-resolution is used. In contrast to the conventional method, the method proposed here gives an estimate on how much systematic change is included in the records, which is not due to long-term correlations. More work needs to be done to understand other types of trends.

5. Summary and outlook

In summary, we have proposed a DFA-based technique to estimate trends in records, where also long-term correlations are present. The method is based on the comparison of the fluctuation functions in DFA0 (which reflects trends) and DFA2 (which systematically removes linear trends). By applying DFA0 and DFA2 to a large number of synthetic records with well defined correlation properties and trends, we were able to estimate the probability that a given long-term correlated record contains a certain trend.

Our approach differs from the one that has been followed in Ref. [42], where the scaling of fit-coefficients of the DFA-regression (which normally are not being considered) has been analyzed. We have used an different approach to identify possible trends in six observational temperature records. We found that the conventional regression method which does not take into account long-term correlations, significantly overestimates the trend, in 3 of 6 cases by about 50 %, in 2 cases by 40 %, and in one case (Vienna) by 5 %. More work with more stations has to be done to confirm this picture. We plan to extend this work also to river flows and precipitation, where the data strongly deviate from Gaussians and non-linear long-term correlations also exist.

Acknowledgments

We would like to thank the German Federal Ministry of Education and Research for financial support. We are very grateful to Ivo Mossig & Ernst Giese for useful discussions. We would like to thank PIK-Potsdam and Anders Moberg for providing the temperature records.

References

[1] H.E. Hurst, Long-term storage capacity of reservoirs, Transactions of the American Society of Civil Engineers 116 (2447) (1951) 770–808.
[2] B.B. Mandelbrot, J.R. Wallis, Noah, Joseph, and operational hydrology, Water Resources Research 4 (5) (1968) 909–918.
[3] B.B. Mandelbrot, J.R. Wallis, Some long-run properties of geophysical records, Water Resources Research 5 (2) (1969) 321–340.
[4] E. Koscielny-Bunde, A. Bunde, S. Havlin, Y. Goldreich, Analysis of daily temperature fluctuations, Physica A 231 (4) (1996) 393–396.
[5] J.D. Pelletier, D.L. Turcotte, Long-range persistence in climatological and hydrological time series: Analysis, modeling and application to drought hazard assessment, Journal of Hydrology 203 (1–4) (1997) 198–208.
[6] E. Koscielny-Bunde, A. Bunde, S. Havlin, H.E. Roman, Y. Goldreich, H.-J. Schellnhuber, Indication of a universal persistence law governing atmospheric variability, Physical Review Letters 81 (3) (1998) 729–732.
[7] P. Talkner, R.O. Weber, Power spectrum and detrended fluctuation analysis: Application to daily temperatures, Physical Review E 62 (1) (2000) 150–160.
[8] R.O. Weber, P. Talkner, Spectra and correlations of climate data from days to decades, Journal of Geophysical Research—Atmospheres 106 (D17) (2001) 20131–20144.
[9] J.F. Eichner, E. Koscielny-Bunde, A. Bunde, S. Havlin, H.-J. Schellnhuber, Power-law persistence and trends in the atmosphere: A detailed study of long temperature records, Physical Review E 68 (4) (2003) 046133.
[10] R.A. Monetti, S. Havlin, A. Bunde, Long-term persistence in the sea surface temperature fluctuations, Physica A 320 (2003) 581–589.
[11] A. Király, I. Bartos, I.M. Jánosi, Correlation properties of daily temperature anomalies over land, Tellus 58A (5) (2006) 593–600.
[12] D. Rybski, A. Bunde, H. von Storch, Long-term memory in 1000 years simulated temperature records, Journal of Geophysical Research—Atmospheres 113 (D2) (2008) D02106.
[13] J.W. Kantelhardt, E. Koscielny-Bunde, D. Rybski, P. Braun, A. Bunde, S. Havlin, Long-term persistence and multifractality of precipitation and river runoff records, Journal of Geophysical Research—Atmospheres 111 (D1) (2006) D01106.
[14] J. Kropp, H.-J. Schellnhuber (Eds.), In Extremis: Trends, Correlations, and Extremes in Hydrology and Climate, Springer-Verlag, Berlin, 2009 (in press).
[15] P.C. Ivanov, A. Bunde, L.A.N. Amaral, S. Havlin, J. Fritsch-Yelle, R.M. Baevsky, H.E. Stanley, A.L. Goldberger, Sleep-wake differences in scaling behavior of the human heartbeat: Analysis of terrestrial and long-term space flight data, Europhysics Letters 48 (5) (1999) 594–600.
[16] A. Bunde, S. Havlin, J.W. Kantelhardt, T. Penzel, J.H. Peter, K. Voigt, Correlated and uncorrelated regions in heart-rate fluctuations during sleep, Physical Review Letters 85 (17) (2000) 3736–3739.
[17] F. Lux, M. Ausloos, Market fluctuations I: Scaling, multiscaling, and their possible origins, in: The Science of Disasters, Springer-Verlag, Berlin, 2002, pp. 373–409 (chapter 13).
[18] R.N. Mantegna, H.E. Stanley, An Introduction to Econophysics: Correlations and Complexity in Finance, Cambridge University Press, Cambridge, 1999.
[19] P. Ivanov, K. Hu, M. Hilton, S. Shea, H.E. Stanley, Endogenous circadian rhythm in human motor activity uncoupled from circadian influences on cardiac dynamics, Proceedings of the National Academy of Sciences of the United States of America 104 (52) (2007) 20702–20707.
[20] D. Rybski, S.V. Buldyrev, S. Havlin, F. Liljeros, H.A. Makse, Emergent laws of human interaction activity, preprint.
[21] D. Rybski, A. Bunde, S. Havlin, H. von Storch, Long-term persistence in climate and the detection problem, Geophysical Research Letters 33 (6) (2006) L06718.
[22] A. Bunde, J.F. Eichner, J.W. Kantelhardt, S. Havlin, Long-term memory: A natural mechanism for the clustering of extreme events and anomalous residual times in climate records, Physical Review Letters 94 (4) (2005) 048701.
[23] J.F. Eichner, J.W. Kantelhardt, A. Bunde, S. Havlin, Statistics of return intervals in long-term correlated records, Physical Review E 75 (1) (2007) 011128.
[24] J.W. Kantelhardt, E. Koscielny-Bunde, H.H.A. Rego, S. Havlin, A. Bunde, Detecting long-range correlations with detrended fluctuation analysis, Physica A 295 (3–4) (2001) 441–454.
[25] T.A. Cohn, H.F. Lins, Nature's style: Naturally trendy, Geophysical Research Letters 32 (23) (2005) L23402.
[26] C.-K. Peng, S.V. Buldyrev, S. Havlin, M. Simons, H.E. Stanley, A.L. Goldberger, Mosaic organization of DNA nucleotides, Physical Review E 49 (2) (1994) 1685–1689.
[27] K. Hu, P.C. Ivanov, Z. Chen, P. Carpena, H.E. Stanley, Effect of trends on detrended fluctuation analysis, Physical Review E 64 (1) (2001) 011114.
[28] Z. Chen, P.C. Ivanov, K. Hu, H.E. Stanley, Effect of nonstationarities on detrended fluctuation analysis, Physical Review E 65 (4) (2002) 041107.
[29] M.S. Taqqu, V. Teverovsky, W. Willinger, Estimators for long-range dependence: An empirical study, Fractals 3 (4) (1995) 785–798.
[30] A. Bashan, R. Bartsch, J.W. Kantelhardt, S. Havlin, Comparison of detrending methods for fluctuation analysis, Physica A 387 (21) (2008) 5080–5090.
[31] J. Kantelhardt, S. Zschiegner, E. Koscielny-Bunde, S. Havlin, A. Bunde, H. Stanley, Multifractal detrended fluctuation analysis of nonstationary time series, Physica A 316 (1–4) (2002) 87–114.
[32] J. Feder, Fractals, Physics of Solids and Liquids, Plenum Press, New York, 1988.
[33] C.-K. Peng, S.V. Buldyrev, A.L. Goldberger, S. Havlin, F. Sciortino, M. Simons, H.E. Stanley, Long-range correlations in nucleotide sequences, Nature 356 (6365) (1992) 168–170.
[34] D. Koutsoyiannis, Nonstationarity versus scaling in hydrology, Journal of Hydrology 324 (1–4) (2006) 239–254.
[35] S. Havlin, R. Blumberg Selinger, M. Schwartz, H.E. Stanley, A. Bunde, Random multiplicative processes and transport in structures with correlated spatial disorder, Physical Review Letters 61 (13) (1988) 1438–1441.
[36] C. Heneghan, G. McDarby, Establishing the relation between detrended fluctuation analysis and power spectral density analysis for stochastic processes, Physical Review E 62 (5) (2000) 6103–6110.
[37] G. Rangarajan, M. Ding, Integrated approach to the assessment of long range correlation in time series data, Physical Review E 61 (5) (2000) 4991–5001.

[38] H. Bergström, A. Moberg, Daily air temperature and pressure series for Uppsala (1722–1998), Climatic Change 53 (1–3) (2002) 213–252.
[39] A. Moberg, H. Alexandersson, H. Bergström, P.D. Jones, Were southern swedish summer temperatures before 1860 as warm as measured?, International Journal of Climatology 23 (12).
[40] S. Lennartz, A. Bunde, Eliminating finite-size effects in short records with long-term memory, preprint.
[41] W. Härdle, Applied Nonparametric Analysis, Cambridge University Press, Cambridge, 1990.
[42] D. Vjushin, R.B. Govindan, R.A. Monetti, S. Havlin, A. Bunde, Scaling analysis of trends using DFA, Physica A 302 (1–4) (2001) 234–243.